Investigation and Modelling of Single-Molecule Organic Transistors

Fabrizio Torricelli[1], Eleonora Macchia[2,3], Paolo Romele[1], Kyriaki Manoli[2], Cinzia Di Franco[4], Zsolt M. Kovacs-Vajna[1], Gerardo Palazzo[2,5,6], Gaetano Scamarcio[4,5], Luisa Torsi[2,3,6]

[1] Department of Information Engineering, University of Brescia, 25123 Brescia, Italy
[2] Dipartimento di Chimica, Università degli Studi di Bari "Aldo Moro", 70125 Bari, Italy.
[3] The Faculty of Science and Engineering, Åbo Akademi University, 20500 Turku, Finland.
[4] CNR, Istituto di Fotonica e Nanotecnologie, Sede di Bari, 70125 Bari, Italy.
[5] Dipartimento InterAteneo di Fisica "M. Merlin", Università degli Studi di Bari "Aldo Moro", 70125 Bari, Italy.
[6] CSGI (Centre for Colloid and Surface Science), 70125 Bari, Italy.

email: fabrizio.torricelli@unibs.it – luisa.torsi@uniba.it

***Abstract*— Biofunctionalized organic transistors have been recently proposed as a simple wide-field single molecule technology. The further development and engineering of this disruptive technology urgently requires the understanding and modelling of the device operation. Here we show a physical-based numerical model of single molecule organic transistors. The model accurately reproduces the measurements in the whole range of protein concentrations with a unique set of parameters. The model provides quantitative information on the bioelectronic device operation. It is an important tool for further development of transistor-based single molecule.**

Keywords—modelling, single-molecule, organic transistor, biosensor

I. Introduction

Single molecule electronic detection is triggering a great deal of attention because it has the potential to revolutionize the current approach to diagnostics. Recently, a label-free single molecule detection technology based on millimeter-sized organic transistors with a gate electrode bio-functionalized with ~10^{12} bio-probes has been proposed [1,2]. Analogously to systems in nature [3,4] single molecule organic transistors (SiMoTs) provides a high interaction cross-section by means of a large number of highly packed receptors. SiMoT technology finds relevant application in several fields, as for example early diagnostic and personalized medicine, where a specific set of biomarkers has to be detected at the lowest concentration possible [5,6]. A low limit of detection, ideally single molecule, is the key for an effective and non-invasive early diagnostic. To meet the needs of these applications, the SiMoT technology has to be integrated in arrays and electronic systems. Moreover, the further development and engineering of the SiMoT technology urgently require a clear investigation and understanding of the impact of the biorecognition event on the device parameters.

In this work, we show a physical-based numerical model of SiMoTs. The electrical characteristics of SiMoTs are accurately reproduced when the ligand concentration ranges from 0 M up to 10^{-13} M with a unique set of physical and geometrical parameters. The model reveals that nano-scale single-protein interaction results in a macro-scale variation of the gate electrode work function measured as a shift of the transfer characteristics. In addition, the model shows that a single binding event affects several binding sites due to a cooperative field-assisted mechanism and quantifies the number of binding sites affected by the protein binding.

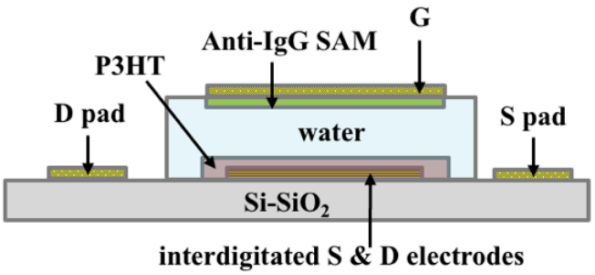

Fig. 1. Schematic side-view of a single-molecule organic transistor (SiMoT).

II. SiMoT Fabrication and Measurements

The SiMoT structure is shown in Fig. 1. Titanium/Gold (5nm / 50nm) source and drain electrodes are evaporated and patterned with photolithography on a Si/SiO_2 substrate. Before the electrodes deposition the Si O_2 surface is carefully cleaned in an ultrasonic bath of acetone and isopropanol for 10 minutes. The transistor channel width and length are W = 12800 μm and L = 5 μm, respectively. Poly(3-hexylthiophene-2,5-diyl) (P3HT) organic semiconductor (OSC) is dissolved in 1,2-dichlorobenzene (2.6 mg/ml), filtered with 0.2 μm PTFE filter, deposited by spin coating at 2000 r.p.m. and patterned (A_{OSC} = 6.4 10^{-3} cm^2) to form the channel. To improve the polymer morphology the devices are annealed 1h on a hot plate at 80 °C. A polydimethylsiloxane well is glued and filled with 300 μl of water (HPLC grade) acting as gating medium. A Kapton foil covered by e-beam evaporated gold is used as a gate (A_G = 0.6 cm^2). The gate is positioned on the top of the water, in front of the transistor channel.

The biofunctionalized gate is obtained by covering a bare Au gate with densely-packed anti-human Immunoglobulin G (anti-IgG). According to the protocol reported in [1], the gate is cleaned in an ultrasonic isopropanol bath for 10 minutes, dried with nitrogen and cleaned with UV/ozone for 10 minutes. The chemical self-assembled monolayer (chem-SAM) is obtained by mixing a 10 mM solution of 10:1 3-MPA to 11-MUA in ethanol. The gate is immersed in the chem-SAM solution overnight in nitrogen. Subsequently, the chem-SAM formed on the gold surface of the gate electrode is

978-1-7281-0940-4/19/$31.00 ©2019 IEEE

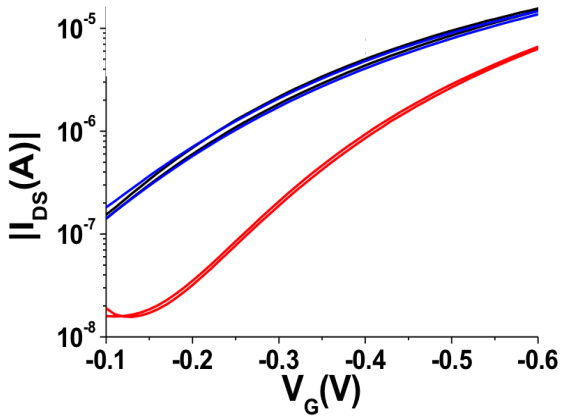

Fig. 2. Measured transfer characteristics of a single molecule transistor (SiMoT) at V_D= -0.4V before (blue and black curves) and after (red curve) biofunctionalization of the gate.

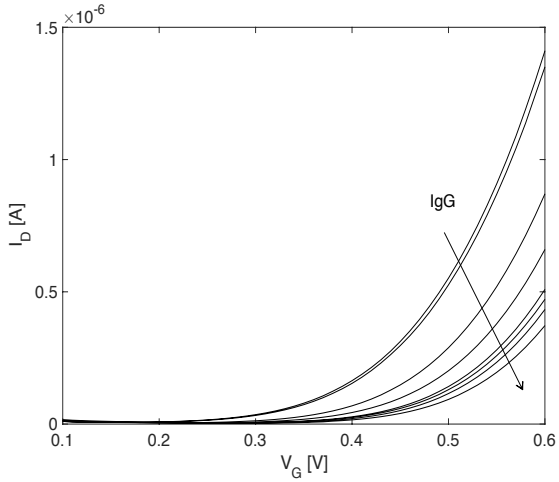

Fig. 3. Measured transfer characteristics of SiMoT at various protein concentrations. V_D= -0.4V.

activated with a solution of 200 mM EDC and 50 mM sulfo-NHS in aqueous solution for 2h. Then the gate is rinsed with PBS and incubated in a solution of phosphate buffer solution (PBS, pH 7.4, KCl 2.7 mM, NaCl 137 mM) with 100 µg/ml of anti-immunoglobulins (anti-IgG) for 2h. The gate is rinsed with PBS and incubate in a PBS solution with 1M ethanolamine in order to block the unreacted sulfo-NHS groups. Finally, the gate is immersed in a PBS solution with 100 µg/ml of BSA for 1h. The covalently bounded anti-IgG and the adsorbed BSA formed the bio-SAM. Typical transfer characteristics measured with a bare Au gate (blue and black curves) and with a biofunctionalized gate before the biosensing are shown in Fig. 2 (red curve). The comparison shows that after the gate biofunctionalization the transfer characteristic shift to more negative voltages, which result in a lower maximum drain current. The transistor with a biofunctionalized gate shows a maximum drain current larger than 6 10^{-6} A and the OFF current is about 2 10^{-8} A, resulting in an ON/OFF current ratio larger than 10^2. This is typical for P3HT electrolyte-gated transistors, thus confirming that the biofunctionalized gate does not negatively affect the transistor performance.

The SiMoT biosensing response is obtained by diluting the IgG protein in PBS at concentrations ranging from 10^{-21} M to 10^{-13} M. The gate is incubated in the analyte for 10 minutes and then measured with SiMoT, according to the SiMoT configuration showed in Fig. 1. Fig. 3 shows the measured transfer characteristics I_D-V_G of a SiMoT sensor as a function of the protein concentration (symbols). We found that the measured drain current reduces by increasing the nominal protein concentration. In addition, as a control experiment we incubated the gate biofunctionalized with anti-IgG with another protein, namely IgM. We found that after incubation of the gate with IgM the transfer characteristic is unaffected, thus proving the bioelectronic selectivity of the SiMoT.

III. SiMoT Model

To investigate the key physical and electrical device parameters, we developed a SiMoT physical model. In high-molecular-weight polymers charge transport occurs through an interconnected network of ordered regions while the amorphous fraction of the film does not participate to the transport. As charges reside in the ordered regions, the structural disorder in these regions define the electronic properties and it can be quantitatively measured by the paracristallinity parameter g. In P3HT g = 3-7% [7] indicating the coexistence of localized and delocalized states: in paracrystalline aggregates the charge is transported by a mechanism where mobile charge is temporarily trapped in localized states, akin the multiple trapping and release [8-10].

According to this physical background, we calculate the drift-diffusion transport equation including a density of states DOS(E) = g_t(E) + g_b(E) where the localized states are described as:

$$g_t = \frac{N_t}{E_t} exp\left(\frac{E-E_{HOMO}}{E_t}\right) \quad (1)$$

Where N_t is the total density of localized states, E_t is the energy disorder, and E_{HOMO} is the highest occupied molecular orbital (HOMO) energy.

The delocalized states are describe as:

$$g_b = \frac{N_{HOMO}}{k_B T}\sqrt{\frac{E-E_{HOMO}}{k_B T}} \quad (2)$$

in the energy range E > E_{HOMO}. N_{HOMO} is the total density of HOMO states, k_B is the Boltzmann constant, and T is the temperature.

The hole density as a function of the Fermi energy level is calculated by solving the Fermi-Dirac integral and reads:

$$p(E_F) = \int_{-\infty}^{+\infty} DOS(E)[1 - f_d(E, E_F)]dE \quad (3)$$

where the DOS is given by the sum of Eq. (1) and Eq. (2), and the Fermi-Dirac distribution reads:

$$f_d(E, E_F) = \frac{1}{1+\exp\left(\frac{E-E_F}{k_B T}\right)} \quad (4)$$

The drift-diffusion transport equation is integrated along the channel length and thickness and results [11,12]:

$$I_D = \frac{W}{L}\int_{V_S}^{V_M}\int_{V_{ch}}^{\varphi_s}\frac{\sigma_0 \exp\left[\frac{q(\varphi-V_{ch})}{k_B T}\right]}{\sqrt{\frac{2q}{\epsilon_s}\int_{V_{ch}}^{\varphi} p(\Psi,V_{ch})d\Psi}} d\varphi dV_{ch} \quad (5)$$

where ε_s the OSC permittivity, σ_0 = q μ_0 N_{HOMO} exp[E_G/(2k_BT)], E_G = E_{LUMO}-E_{HOMO} is the energy gap, μ_0 is the hole mobility in the delocalized states, E_{LUMO} is the lowest unoccupied molecular orbital energy level, q is the elementary charge, φ is the potential, φ_s is the surface potential, V_{ch} is the the Pseudo-Fermi potential. It is worth to note that in Eq. (5)

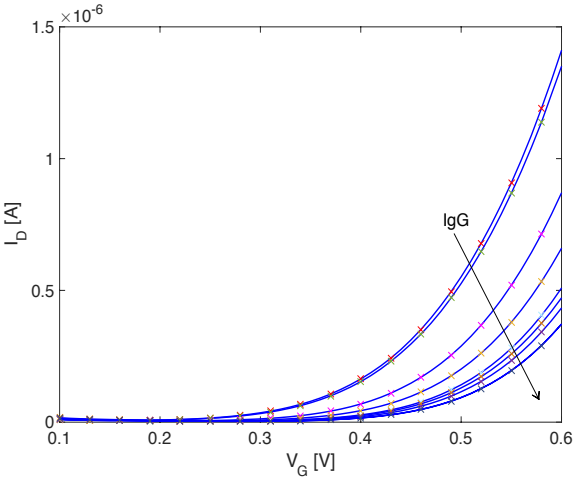

Fig. 4. SiMoT transfer characteristics as a function of IgG concentration. The protein concentration is varied from 6 10^{-21} M to 6 10^{-13} M. Symbols are the measurements, full lines are calculated solving Eqs. (1)-(7).

$E_F = E_{F0} + q\,(\varphi - V_{ch})$, where E_{F0} is the OSC Fermi energy level at equilibrium conditions. $V_M = \min\{V_G - V_T, V_D\}$ V_G is the gate voltage, V_T is the threshold voltage, and V_D is the drain voltage.

Eqs. (1)-(2) are numerically solved by applying the Gauss' law to the water/semiconductor interface. The electric field into the semiconductor can be calculated as:

$$F_x(\varphi_s) = \frac{C_{EDL}}{\epsilon_s}(V_{EL} - \varphi_s) \qquad (6)$$

where $C_{EDL} = \varepsilon_0\,\kappa_w / t_{EDL}$ is the electrolyte/semiconductor electric-double-layer (EDL) capacitance per unit area, κ_w is the relative permittivity of electrolyte, t_{EDL} is the thickness of the EDL at the electrolyte/semiconductor interface, $V_{EL} = (C_G\,A_G / C_T)\,(V_G - V_{FB}) + (C_{EDL}\,A_{OSC} / C_T)\,\varphi_s$, $C_G = (\varepsilon_0\,\kappa_{SAM} / t_{SAM})$ is the gate/ electrolyte capacitance per unit area, κ_{SAM} and t_{SAM} are the relative permittivity and the thickness of the self-assembled monolayer, respectively, and $C_T = C_G\,A_G + C_{EDL}\,A_{OSC}$.

The measured capacitances is equal to $C'_G = C_G\,A_G = 6$ µF and $C'_{OSC} = C_{OSC}\,A_{OSC} = 69$ nF and therefore V_{EL} can be approximated as $V_{EL} \approx (C_G\,A_G / C_T)\,(V_G - V_{FB})$, where V_{FB} is the SiMoT threshold voltage and it accounts for the biofunctionalized gate work-function, the electrochemical potential of the electrolyte (in our case water) and the equilibrium Fermi energy of the OSC.

Finally, φ_s can be calculated from the continuity of the displacement at the electrolyte-semiconductor interface:

$$\frac{C_{OSC}}{\varepsilon_s}(V_G - V_{FB} - \varphi_s) = \sqrt{\frac{2q}{\epsilon_s}\int_{V_{ch}}^{\varphi} p(\Psi, V_{ch})\,d\Psi} \qquad (7)$$

The integral expression (5) coupled with the electrolyte/semiconductor boundary condition (7) are numerically solved for each set $\{V_G, V_D, V_S\}$ and the drain current of SiMoT is calculated.

IV. Results and Discussion

Fig. 4 shows the comparison between the measurements and the model. Eqs. (1)-(7) accurately reproduces the drain current measured by varying the nominal ligand concentration with a single set of geometrical and physical parameters. More

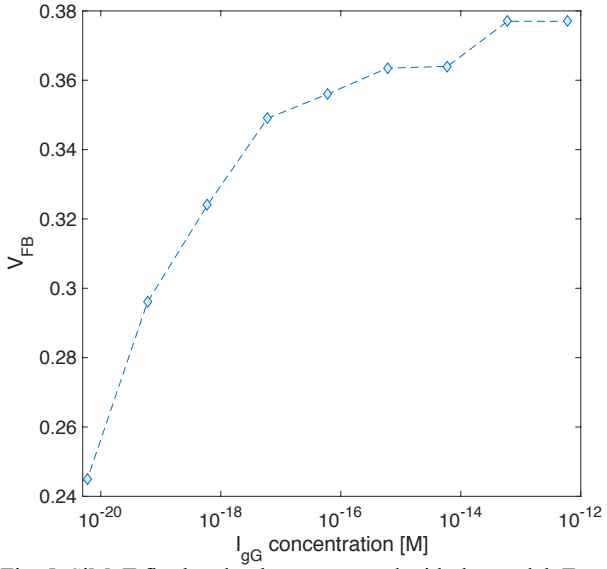

Fig. 5. SiMoT flat-band voltage extracted with the model, Eqs. (1)-(7), as a function of the nominal protein concentration IgG, which ranges from 6 10^{-21} M to 6 10^{-13} M.

in detail, the model parameters are obtained as follows. W, L, A_{OSC}, A_G, and T are measured. $\varepsilon_s = 3\,\varepsilon_0$, $E_{LUMO} = 3.2$ eV, and $E_{HOMO} = 5.1$ eV are taken from [13]. The total density of states $N_{HOMO} = 1.28\ 10^{20}$ cm^{-3} is taken from the density functional theory calculations [14]. The EDL capacitance at the water/semiconductor interface $C_{EDL} = 7.5$ µF cm^{-2} was measured by means of electrochemical impedance spectroscopy. By fitting a single transfer characteristic measured after incubation with PBS with the drain current model Eqs (1)-(7) we obtained $\mu_0 = 0.058$ cm^2 V^{-1} s^{-1}, $N_t = 1.75\ 10^{20}$ cm^{-3}, $E_t = 72\ 10^{-3}$ eV, and $V_{FB} = 0.237$ V. It is worth noting that, according to [7], the extracted E_t yields a paracristallinity g ~ 5%, which is fully consistent with the multiple trapping and release transport model here used.

We used the model to predict the drain current of SiMoTs as a function of the protein concentration. As shown in Fig. 4 the model (lines) accurately predicts the measurements (symbols) in the whole range of gate voltages and ligand concentrations. By varying the protein concentration, we found that only V_{FB} changes (Fig. 5) while all the other model parameters are the same. Since the biorecognition takes place at the surface of the gate electrode in contact with water, the variation of the flat-band voltage can be attribute to a variation of the gate work function that, in turn, is caused by a redistribution of charge along the bioprobes immobilized to the gate. Fig. 5 shows that V_{FB} significantly changes when the protein concentration is in the range 6 10^{-21} M to 6 10^{-18} M while at larger concentrations a modest response is shown and at IgG concentrations larger than 6 10^{-13} M V_{FB} becomes constant. The flat-band saturation obtained when the incubated in PBS with a large number of IgGs is readily explained by considering that at large protein concentrations all the binding sites available on the gate have been affected by the various biorecognition events.

We can estimate the fraction (η) of binding sites immobilized on the gate affected by the biorecognition at a given concentration as: $N_{bioprobes} = \eta\,A_G / A_{anti\text{-}IgG}$, where $A_{anti\text{-}IgG} = 100$ nm^2 is the average area of a bioprobe obtained by means of surface plasmon resonance measurements and η is calculated by solving the following equation: $V_{FB}(c) = V_{FB0}\,(1 - \eta) + V_{FBmax}\,\eta$, where $V_{FB}(c)$, V_{FB0} and V_{FBmax} are V_{FB}

obtained with the model after incubation at the protein concentration c, in PBS and at the maximum concentration (viz. 6 10^{-13} M), respectively. We found that about the 40% of the binding sites are affected by a single biorecognition event and the incubation of the biofunctionalized gate with tens of IgG proteins affects more than 60% of the binding sites.

The single-molecule sensitivity of the SiMoT could be explained by considering a cooperative effect taking place on the highly-packed SAM [1]. It is well known that the antigen/antibody binding is an exothermic reaction and the energy of the anti-IgG/IgG reaction is of the order of kJ/mol [15]. Therefore, it is reasonable to assume that part of this huge energy is transferred from the bio-SAM to the chem-SAM after a biorecognition event, and this results in a local desorption of the alkanethiols. By considering that after the ethanolamine functionalization step a hydrogen-bonding network is formed in the chem-SAM, the local defect can be propagated under the effect of the gate electric field. This results in a variation of the dipole orientation over several micrometer-square area of the gate and reflects in an appreciable variation of the gate work-functions which, in turn, is displayed by the SiMoT flat-band voltage.

V. Conclusion

A physical-based numerical model of single molecule organic transistors is proposed. The measured transfer characteristics are accurately described in the whole wide-range of protein concentration assessed. The physical and material bio-transistor device parameters are obtained. The model shows that the biorecognition events results in a variation of the transistor flat-band voltage, which enables the quantification of the number of bioprobes anchored to the gate involved in the biorecognition process. The proposed model is a valuable tool for the understanding, simulation and further development of the SiMoT technologies, including for example multi-modal biomarker assays and array integration.

Acknowledgment

The authors would like to acknowledge the financial support of the European Commission for the projects SiMBiT (Horizon 2020 ICT, contract n°824946).

References

[1] E. Macchia et al., “Single-molecule detection with a millimitre-sized transistor,” Nat. Commun., vol. 9, no. 3223, pp. 1-10, Aug. 2018. DOI: 10.1038/s41467-018-05235-z.

[2] E. Macchia et al., “Label-Free and Selective Single-Molecule Bioelectronic Sensing with a Millimeter-Wide Self-Assembled Monolayer of Anti-Immunoglobulins,” Chem. Mater., Article early access, Jan 2019. DOI: 10.1021/acs.chemmater.8b04414

[3] T. Strünker, et al., “A K^+-selective cGMP-gated ion channel controls chemosensation of sperm,” Nat. Cell Biol., vol. 8, pp. 1149-1154, Jul. 2006. DOI: 10.1038/ncb1473

[4] T. Leinders-Zufall, et al., “Ultrasensitive pheromone detection by mammalian vomeronasal neurons,” Nature, vol. 405, 792-796, Jun. 2000. DOI: 10.1038/35015572

[5] S. Sorgenfrei, et al., “Label-free single-molecule detection of DNA-hybridization kinetics with a carbon nanotube field-effect transistor,” Nat. Nanotechnol., vol. 6, pp. 126-132, Jan. 2011. DOI: 10.1038/nnano.2010.275

[6] J. K. Rosenstein, S. G. Lemay, and K. L. Shepard “Single-molecule bioelectronics,” Nanomed. Nanobiotechnol., vol.7, pp. 475-493, Dec. 2015. DOI: 10.1002/wnan.1323

[7] R. Noriega, et al., “A general relationship between disorder, aggregation and charge transport in conjugated polymers,” Nat. Mater., vol. 12, pp. 1038-1044 Aug. 2013. DOI: 10.1038/nmat3722

[8] J. F. Chang, H. Sirringhaus, M. Giles, M. Heeney, and I. McCulloch, “Relative importance of polaron activation and disorder on charge transport in high-mobility conjugated polymer field-effect transistors,” Phys. Rev. B, vol. 76, no. 20, pp. 205204, Nov. 2007. DOI: 10.1103/PhysRevB.76.205204

[9] F. Torricelli, L. Colalongo, L. Milani, Zs. M. Kovács-Vajna, and E. Cantatore, “Impact of energetic disorder and localization on the conductivity and mobility of organic semiconductor,” IEEE 2011 Int. Conf. on Simul. of Semicon. Proc. and Devices (SISPAD), no. 12289431, Sep. 2011. DOI: 10.1109/SISPAD.2011.6035084

[10] Y. Yamashita, et al., “Transition Between Band and Hopping Transport in Polymer Field‐Effect Transistors,” Adv. Mater., vol. 26, pp. 8169-8173, Oct. 2014. DOI: 10.1002/adma.201403767

[11] F. Torricelli, “Charge Transport in Organic Transistors Accounting for a Wide Distribution of Carrier Energies – Part I: Theory,” IEEE Trans. Electron Devices, vol. 59, no. 5, pp. 1514-1519, May 2012. DOI: 10.1109/TED.2012.2187830

[12] F. Torricelli, K. O'Neill, G. H. Gelinck, K. Myny, J. Genoe, and E. Cantatore, “Charge Transport in Organic Transistors Accounting for a Wide Distribution of Carrier Energies – Part II: TFT Modeling,” IEEE Trans. Electron Devices, vol. 59, no. 5, pp. 1520-1528, May 2012. DOI: 10.1109/TED.2012.2184764

[13] K. Hong, S. H. Kim, A. Mahajan, and C. D. Frisbie, “Aerosol Jet Printed p- and n-type Electrolyte-Gated Transistors with a Variety of Electrode Materials: Exploring Practical Routes to Printed Electronics,” ACS Appl. Mater. Interfaces, vol. 6, no. 21, pp. 18704-18711, Oct. 2014. DOI: 10.1021/am504171u

[14] J. E. Northrup, “Atomic and electronic structure of polymer organic semiconductors: P3HT, PQT, and PBTTT,” Phys. Rev. B, vol. 76, no. 24, pp. 245202, Dec. 2007. DOI: 10.1103/PhysRevB.76.245202

[15] M. Oda, K. Kozono, H. Mori, and T. Azuma, “Evidence of allosteric conformational changes in the antibody constant region upon antigen binding,” Int. Immunol. 15, 417-426 (2003). DOI: 10.1093/intimm/dxg036